A Low Cost Environmental Ionizing Radiation Detector Based on COTS CMOS Image Sensors

Clara Lucía Galimberti*[1], Fabricio Alcalde Bessia*‡§[2], Martín Pérez*§, Mariano Gómez Berisso*‡§, Miguel Sofo Haro*‡§, Iván Sidelnik†‡§, Jerónimo Blostein†‡§, Hernán Asorey*‡ and Jose Lipovetzky*‡§[3]

[1]clara@fceia.unr.edu.ar [2]falcalde@ib.edu.ar [3]lipo@ib.edu.ar

*División Bajas Temperaturas y Departamento de Física Médica, Centro Atómico Bariloche, CNEA
Bustillo 9500, San Carlos de Bariloche (8400), Argentina

†División Mediciones Nucleares, Centro Atómico Bariloche, CNEA
Bustillo 9500, San Carlos de Bariloche (8400), Argentina

‡CONICET

§Instituto Balseiro

***Abstract*—We present the development of a system for the detection of ionizing radiation based on the Omnivision OV5647 Commercial Off The Shelf image sensor. The data is read and processed in real-time using a Raspberry Pi 3 computer. The amount of charge and geometrical characteristics of the cluster of pixels exited when a particle interacts with the sensor is recorded and used to identify the type of incoming particle, distinguishing between alpha particles and X-ray or gamma photons. The software was programmed in C using the OpenCV library. The system was tested with ^{137}Cs and ^{241}Am radiation sources.**

Resumen **Se presenta el desarrollo de un sistema para la detección de radiación ionizante basado en el sensor comercial de imagen Omnivision OV5647. Los datos obtenidos con el detector son leídos y procesados en tiempo real usando una computardora Raspberry Pi 3. La cantidad de carga y características geométricas del cluster de pixeles exitado cada vez que una partícula interactúa con el sensor es usado para estimar el tipo de partícula incidente diferenciando entre partículas alfa, y fotones gamma o de rayos X. El software fue programado en C usando la librería OpenCV. El sistema fue testeado utilizando fuentes radioactivas de ^{137}Cs y ^{241}Am.**

I. Introduction

The detection of environmental ionizing radiation is of great importance to detect contamination with radioactive materials and control the Total Ionizing Dose (TID) exposition of workers. For example, the development low-cost accessible radiation detectors was of great importance in Japan after Daiichi nuclear power plant accident, allowing people to own their own and simple detector to monitor the background radiation in their houses. Ref. [1] presents the development of the PoKeGa, an inexpensive detector based on PIN photodiodes that generates a signal which can be acquired using the microphone jacket of a cell phone. The detector allows the detection of gamma rays at rates from 0.5 tp 10 mSv/h. During the first six months after the Fukushima accident, 12,000 units of the PoKeGa detector were shipped, allowing the collaborative work of almost 2,000 users which shared measurement data. On the other hand, the SafeCast project [2] developed geiger-tube-based detector which comprises a GPS receiver and saves the location of the measurement. The detector, mounted on different vehicles allowed the collaborative collection of data by citizens creating a dose-rate geographical distribution map of the affected region, and with the years of a many countries [3].

In this work, we present a first prototype of a environmental radiation detector based on Commercial Off The Shelf (COTS) image sensors acquired using a low cost RaspBerry Pi board. The data obtained with the sensor can be remotely read using an internet browser. Unlike the PoKeGa and SafeCast projects, the system is oriented to very low dose rates environments, and to the detection not only of gamma photons but also of alpha particles, taking in advantage the characteristics of the detector and the particle classification technique proposed in [4]. The ability to detect and classify alpha particles allows the detection of contaminants for example from the decay-chain of U.

Several works dealt with the use of COTS image sensors as ionizing radiation detectors. In [4], [5] it was shown that the sensor's sensitivity is suitable for personal dosimetry. Ref [6] shows their potential use in the dosimetry of personal exposed to radiation during interventional radiology. The ability to detect thermal neutrons using conversion materials was also shown [7].

The next section shows the implementation of the detection system. It shows how the prototype is built and some interesting characteristics of the image sensor that was used. A brief explanation of the image processing and how the particles are detected is also presented. In section III some experiments were done that show that the prototype is able to detect ionizing particles, and that it allows the classification between different types of particles. Finally, section IV present the conclusions of the work.

II. Implementation

The prototype, shown in Figure 1, was developed using a *Raspberry Pi 3* and an OmniVission OV5647 sensor. The sensor is connected to the Raspberry Pi using the standard

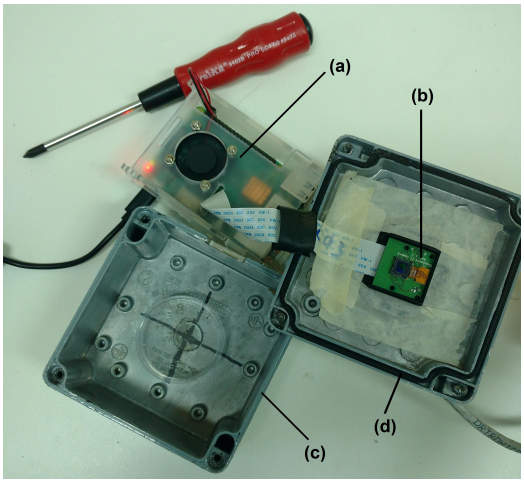

Fig. 1. Detector prototype. (a) *Raspberry Pi 3*, (b) OV5647 sensor, (c) Aluminium box, (d) Light seal.

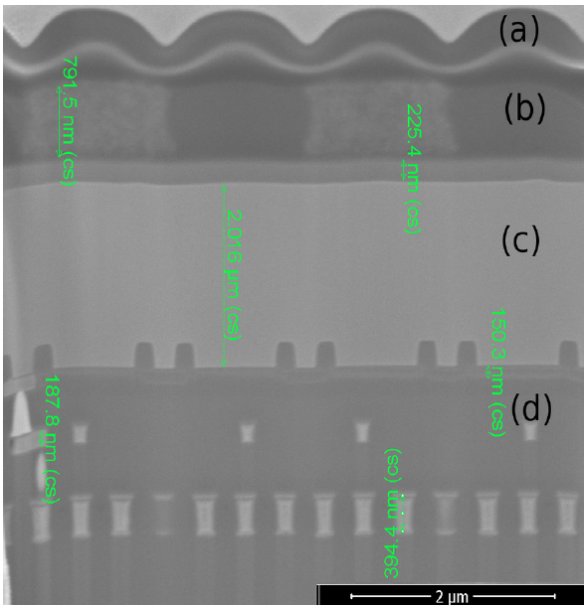

Fig. 2. Cross section of the sensor obtained with a Focus Ion Beam and a Scanning Electron Microscope at 5 kV and 0.20 nA. The layers from top to bottom are: the microlens of each pixel (a), the color filter (b), the active Si volume (c), and insulating layers between metal levels of the integrated circuit (d). After [9].

flex cable as shown in Figure 1, and the communication between them is carried out using I^2C protocol.

The OV5647 is a back-side illuminated (BSI) CMOS image sensor. Unlike traditional image sensors, the BSI sensors are developed in order to receive the radiation from the back-side by flipping the silicon wafer in the manufacturing process. This technique increases the fill factor—i.e. the ratio of photosensitive area to the total pixel area—, reduces the readout noise and consequently improves the low-light performance.

The 5 MPixel sensor contains an array of 2592×1944 pixels with pixel pitch of $1.4\,\mu\mathrm{m}$ x $1.4\,\mu\mathrm{m}$ and image area of $3.7\,\mathrm{mm}$ x $2.7\,\mathrm{mm}$. Figure 2 shows a SEM (Scanning Electron Microscope) image of the die cross-section, which was taken by digging a trench in the pixel array area using a FIB (Focused Ion Beam). It can be seen a layer with microlenses on top of the sensor, which is the backside of the original thinned silicon wafer. Below microlenses there is a $0.8\,\mu\mathrm{m}$ thick Bayer color filter; a small insulating oxide, and then the $2\,\mu\mathrm{m}$ thick Silicon active volume, where the charges produced by ionizing particles will be detected. Finally, below the active volume there are metal interconnection and more insulating layers.

Even though the sensor has a Bayer color filter on top of the sensitive area, the color capability will not be used in this work and the information from all pixels are treated in the same way from the raw data. As will be seen below, the thin layers interposed between the sources and the active volume—i.e. microlenses, color filter and first insulating oxide—are thin enough to be crossed by alpha particles. Also, these layers present a negligible interaction with the photons due to their thickness, much smaller than the several centimeter typical attenuation lengths of the gamma rays used in this work [8]. The same detector was successfully used for acquisition of X-ray images with a high spatial resolution [9].

The operating principle is based on the detection of ionizing particles by searching the image for clusters of bright pixels, which are produced by the ionization in the silicon active volume. First, the image sensor must be isolated from visible light. When a ionizing particle, e.g. a gamma ray, a beta electron, an alpha particle, etc., passes through the sensor, free carriers are produced along its path [4]. These free carriers are then collected by reverse biased P-N junctions of photodiodes and they produce a signal at the output of each pixel in the path of the particle. The more charge generated and collected, the brighter the pixels will be seen in the output image. Every interaction will be an *ionization event* (or *event*). It is possible to detect when an ionizing particle interacts with the sensor by looking at those clusters of bright pixels in the image. Furthermore, the digital values read of those pixels are proportional to the charge collected by each pixel, and so the sum of those digital values is proportional to the total ionization charge produced by the particle in the active volume.

The Raspberry Pi was used to run a program that periodically reads an image from the sensor and processes it as soon as it is available. The image processing algorithm was programmed in C language using the OPENCV [10] library and it is able to detect every event that appears in the image and also calculates some parameters of interest, like the area, charge and image moments. The output of the system are these parameters, explained in the next section, along with a timestamp. This enables the possibility to do some statistical analysis of the events and also enables the use of a event classification criteria.

In order to capture an image, a customized version of the software `raspiraw` [11] was used. It allows the reading of image raw data, which differs considerably from simple unencoded captures. Raw data is the data recorded by the camera's sensor prior to any GPU processing including auto white-balance, vignette compensation, smoothing, downscaling, etc [11]. Moreover, this software gives total control of the sensor registers, allowing the user to set different parameters, such as analog APS gain or exposure time.

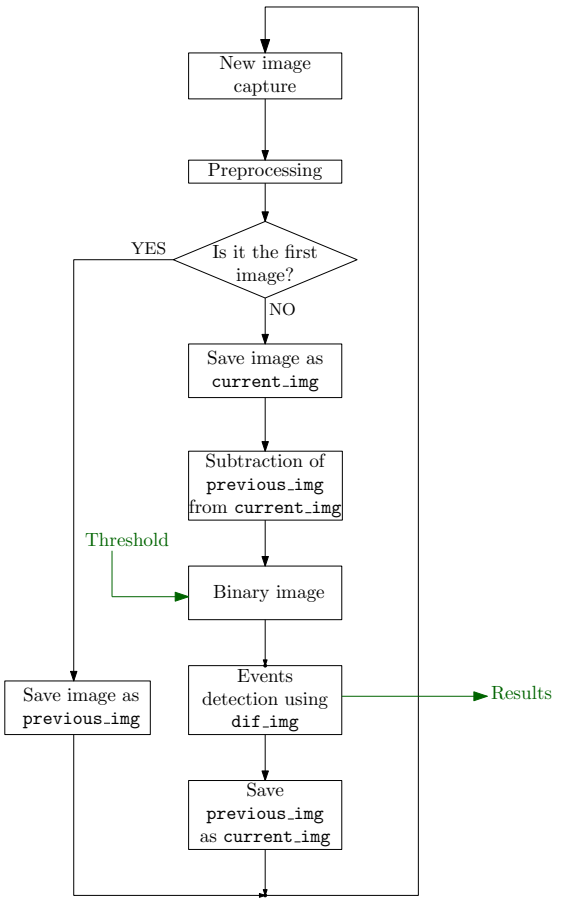

Fig. 3. Algorithm flowchart.

A. Image Processing Algorithm

To reduce the amount of information stored in the system, the images are processed immediately after being acquired, saving only information about the events detected. The algorithm starts when a new image is received. A flowchart resuming all the actions done by the algorithm is presented in Figure 3.

Firstly, the data received is formatted in order to proceed with the analysis, this is called *Preprocessing*. Since the sensor raw data has a digital resolution of 10-bits and it is presented in the software in a packed form—i.e. four 8-bit values, followed by the least-significant 2-bits of those 4 values packed into a fifth byte—and since OPENCV works with 8-bit data, the last two bits of each pixel were dropped. So, the preprocessing stage consists basically in dropping the fifth byte of every 5-byte block. In addition, there are some auxiliary pixels which are used for black level calibration and interpolation as shown in [12] and those are also dropped.

Then, the data is compared with the previous image by doing a subtraction between them in order to eliminate the *fixed-pattern noise* and this result is saved to be used in the following steps. The fixed-pattern noise is a type of noise that appears in the image usually due to damaged pixels. These damaged pixels can be produced for example by radiation [13], [14]. Damaged pixels can have a high baseline level, which if not eliminated could be wrongly taken as a radiation event. The substraction of two consecutive frames assumes that two different events will not occur in the same pixel, assumption reasonable taking in account that typical count rates are of few events per second in the whole image.

Once the image has been preprocessed (or formatted) and the Fixed-Pattern Noise has been eliminated, the event detection takes place. For this purpose, a binary image is created by applying a threshold that was previously determined, and that will be explained in section II-B. The pixels that are over the threshold are set to '1' and the pixels below are set to '0'. Then, this binary image is analyzed and the groups of '1's are identified. These groups correspond to events in the last acquired image. So, by applying this binary mask to the last image the events can be extracted. It is also assumed that the particle flux is low, so two events captured in the same image do not coincide on the same pixels.

Finally, when the events are recovered, the following characteristics are calculated:

- **Area:** Number of pixels affected by the detected event.
- **Charge:** Sum of the digital values of the pixels affected by the detected event. The pixel value is proportional to the voltage sensed which is also proportional to the collected charge, which in turn is related to the charge produced by the ionizing particle. The charge parameter will be given in arbitrary units ([a.u.]) due to the analog-to-digital conversion.
- **Image moments:** Weighted averages of the image pixels intensities which are helpful for calculating different chacarteristics as image centroid and orientation. All the image moments of the event up to the third order are calculated. This information is useful for classification by shape or fast identification of particles with a small grazing angle.

The image moments were calculated as:

$$M_{ij} = \sum_x \sum_y x^i \, y^j \, I(x,y)$$

$$\mu_{pq} = \sum_x \sum_y (x - \bar{x})^p \, (y - \bar{y})^q \, I(x,y)$$

where $I(x,y)$ is the image pixels intensity, M_{ij} are the 'raw' moments and μ_{pq} are the central moments. All indices go from 0 up to 3 (third order moments).

B. Threshold Level Equalization

The pixel photodiode voltage variation—and thus its reading—does not only occur only due to the arrival of a ionizing particle, it also decreases due to the small reverse leakage dark current, providing a low but non zero baseline level in each pixel. The average value of this baseline level is removed with the frame to frame subtraction. But, the randomness generated by the shot noise of the dark current, plus the noise introduced by the analog amplification and digitalization stages inside the chip, provide sources of noise which is observed in dark images. Moreover, the random telegraph signals in damaged pixels can provide higher levels of dark noise even after frames substraction [13]. In order to consider these sources of noise, and differentiate them from a particle-induced event, a threshold should be set for particle detection.

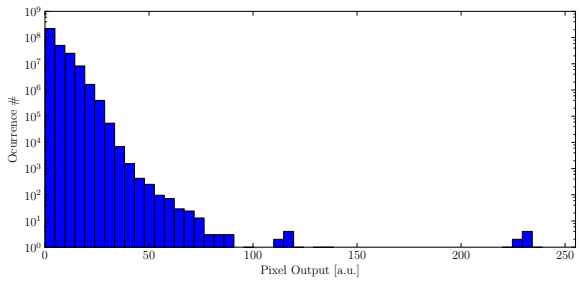

Fig. 4. Histogram of the pixel values of an image taken without any radioactive sources at room temperature. The sensor gain and the exposure time were set to their maximum. The few pixels with values higher than 100 correspond to background radiation events recorded during the measurement.

To do so, sixty dark images were obtained and analyzed. Figure 4 shows the histogram of the values of the difference between pairs of consecutive frames, i.e. a histogram of the noise of the pixels sensor after subtraction. Only positive values are presented. The histogram was fitted with a normal distribution and the resulting standard deviation was 8 digital units. Nevertheless, it was seen that there were a few pixels that deviated a bit from the distribution, possibly due to a bigger noise in a region of the image array (this is without taking into account the few pixels with background radiation events). So, we choose an arbitrary threshold of 120, which is 15 standard deviations away from the mean value, to ensure that the probability of occurrence of a pixel having a value greater than the threshold due to noise is negligible.

III. Measurements and Results

The prototype was tested using two low activity radiation sources, ^{137}Cs and ^{241}Am, which are intended for calibration of instruments. ^{137}Cs is an unstable element with half-life of 30 years and it decays by beta emission in ^{137}Ba, which in turn emits a gamma ray with an energy of 661 keV. Only the gamma rays leave the source due to a thin shielding to stop the beta particles. The activity of this source was 179 kBq the day of the experiment.

On the other hand, ^{241}Am has a half-life of 432 years and it decays emitting alpha particles with an energy of 5.48 MeV and gamma rays of 59 keV. This source had an activity of 2 kBq.

The sources were placed inside the Aluminium box of figure 1, one at a time, and the box was closed to maintain dark conditions. The distance between the source and the image sensor was from 10 mm to 15 mm, small enough to allow alpha particles to reach the sensor. Images were acquired during 37 minutes with the Cesium source and during 4 minutes with the Americium source.

In all cases the OV5647 registers were configured to set the exposure time to its maximum value, as well as the gain also set to its maximum value of 1023. The following section presents a few examples of events captured with each source and statistics of the parameters, like area and charge, recorded during the whole experiment.

A. ^{137}Cs *Experiment*

Figure 5 shows a some examples of the events that were detected while exposing the sensor to the ^{137}Cs source.

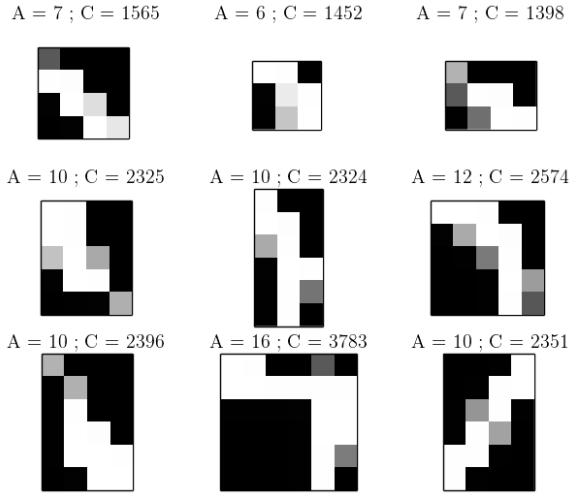

Fig. 5. A few examples of the events detected by the system when exposed to the ^{137}Cs radiation source. White pixels are saturated and correspond to the maximum collected charge, whereas black pixels were not discharged. On top of each image the (C)harge [a.u.] and (A)rea [pixels] parameters, as calculated by the processing algorithm, are shown. The sensor gain was set to its maximum value.

These images correspond to the charge collected by those pixels during the interaction of gamma rays with the silicon active layer. Although these are a few examples only, it can be seen that frequently the particles leave *trace* like events, that is, the images have an elongated shape, and also most pixels are saturated. Due to its energy, the most probable interaction is Compton scattering, and these traces are produced by the Compton electrons released in the interaction [4].

The area and charge parameters where obtained and recorded for all the events detected. Fig. 6 shows histograms of the charge and area of the events during ^{137}Cs irradiation. Due to pixels saturation, both histograms have very similar distributions. Since the active region is very thin, 2μm as seen in figure 2, most of the interactions leave only a fraction of the gamma energy in the sensor.

During the experiment a total number of 2025 events were detected.

B. ^{241}Am *Experiment*

The experiment was repeated using the ^{241}Am alpha source. Again a few examples of the events detected are shown in figure 7. This time there are some rounded events with a big area footprint and charge in the order of tens of thousands, and some others that are smaller and with area and charge parameters similar to the ^{137}Cs events of figure 5. The big and rounded events correspond to alpha particles impinging the sensor, whereas the smaller ones appear due to interactions of Americium gamma rays with Silicon.

This is because the Linear Energy Transfer (LET) of Alpha particles is very high, since these are heavy and charged particles and their interaction is primarily by Coulomb forces. On the other hand, Americium gamma rays deposit their energy by photoelectric effect or Compton scattering, and also their energy is lower than the alpha energy.

The histograms of figure 8 show again the occurrence of each value for area and charge parameters, and for all

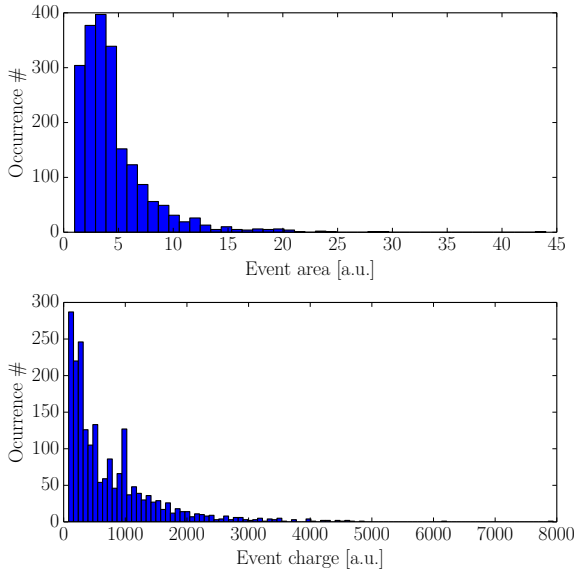

Fig. 6. Histograms of Area and Charge parameters showing the occurrence of each value. Data from the ^{137}Cs experiment. Gain = max.

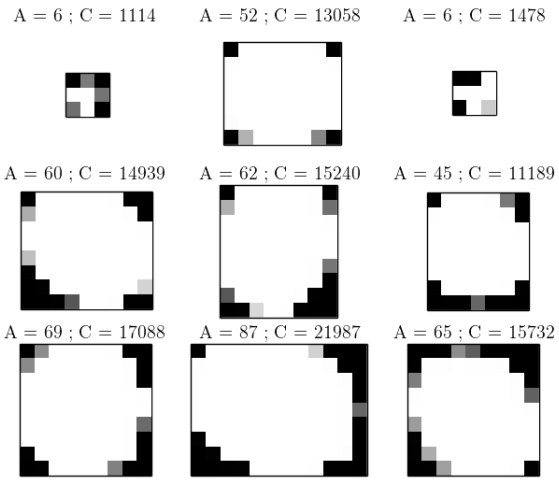

Fig. 7. A few examples of the events detected by the system when exposed to the ^{241}Am radiation source. White pixels are saturated and correspond to the maximum collected charge, whereas black pixels were not discharged. On top of each image the (C)harge [a.u.] and (A)rea [pixels] parameters, as calculated by the processing algorithm, are shown.

the events captured during the exposure of the sensor to the ^{241}Am source. As was observed with the ^{137}Cs source, since most pixels get saturated in the interaction, both histograms have a similar distribution. This saturation was observed even if the pixel gain is reduced, indicating that the full well capacity of the pixel is filled.

Unlike Cesium histograms, in this case there are two distributions clearly marked. The events with area less than 20 units and charge less than 5000 units are produced by the Americium gamma rays, whereas the rest of the events are produced by Alpha particles. These histograms show that it is possible to classify events in Alpha and Not-Alpha through the area or charge parameters. This result is similar to what was observed in [4].

The total number of events detected in this experiment was 1112, of which 350 can be classified as Alpha particles, taking as classification criteria charge higher than 5000. The

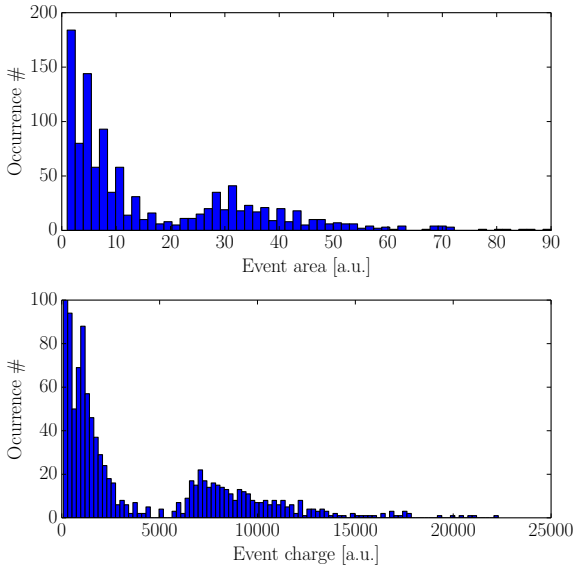

Fig. 8. Histograms of Area and Charge parameters showing the occurrence of each value. Data from the ^{241}Am experiment. Gain = max.

high number of photons detected might include low energy Bremsstrahlung photons generated when alpha particles interact with the first layers of the sensor.

IV. Discussion and Conclusion

Throughout this work a description and characterization of a radiation detector prototype has been presented. The detector is based on a low cost CMOS image sensor and a low cost small computer, which is powerful enough to process the information in real-time.

A image processing algorithm was developed using the OPENCV library, which was able to identify and extract the ionization events from the captured images. Also, the algorithm was programmed to calculate some parameters of interest, like the area of the event, the charge deposited and image moments, that are useful for event classification.

In previous works we used to save the captured images in a video file, and then, in a post-processing step, the whole video file was analyzed looking for ionization events. In a low radiation environment this produces a huge amount of information with only a small useful fraction. The system presented in this work, thanks to the real-time analysis of the captured images, allows to take very long captures—weeks or even months—recording only the parameters of interest of events. Therefore, the analysis of the produced information takes less time and processing power.

It was also observed that alpha particles and gamma photons produce, with the maximum gain, a saturation of the readings of the exited pixels. It is accepted that the energy used to generate an electron-hole pair in Si is 3.6 eV. The full well capacity of the pixels of the sensor is aproximately 4300 electrons [12]. Taking this in account, the energy required to saturate the voltage shift—and thus the reading in each pixel—is aproximately 15.5 keV. This energy is much smaller than the energy deposited by the alpha particles in the active volume of the detector, which explains why even with low gains the pixel response during alpha particle irradiation always saturates.

Thanks to the use of a CMOS image sensor as a radiation detector, it was shown that the system is able to classify the events in Alpha and Not-Alpha. In the presented results, only the charge parameter was used as classification criteria since both area and charge were correlated due to pixel saturation. However, adjusting the sensor gain, it would be possible to develop a more intelligent criteria based not only on charge and area, but also in image moments. The possibility of discrimination between Alpha and Not-Alpha is a very important result since it will allow to measure contaminants coming from the decay chain of Uranium.

ACKNOWLEDGMENT

The authors would like to thank to the RA6 staff for the use of radioactive sources and the Instituto Nacional de Tecnología Industrial for the use of the Focus Ion Beam. This work was done supported by grant PICT 2014-1966, UnCuyo C018, and the Balseiro Institute Summer Grants program.

REFERENCES

[1] Y. Ishigaki, Y. Matsumoto, R. Ichimiya, and K. Tanaka, "Development of mobile radiation monitoring system utilizing smartphone and its field tests in fukushima," *IEEE Sensors Journal*, vol. 13, no. 10, pp. 3520–3526, Oct 2013.

[2] A. Brown, P. Franken, S. Bonner, N. Dolezal, and J. Moross, "Safecast: successful citizen-science for radiation measurement and communication after fukushima," *Journal of Radiological Protection*, vol. 36, no. 2, p. S82, 2016. [Online]. Available: http://stacks.iop.org/0952-4746/36/i=2/a=S82

[3] S. Project. SafeCast live map. [Online]. Available: http://safecast.org/tilemap/

[4] M. Pérez, J. Lipovetzky, M. S. Haro, I. Sidelnik, J. J. Blostein, F. A. Bessia, and M. G. Berisso, "Particle detection and classification using commercial off the shelf CMOS image sensors," *Nuclear Instruments and Methods in Physics Research Section A: Accelerators, Spectrometers, Detectors and Associated Equipment*, vol. 827, pp. 171 – 180, 2016. [Online]. Available: http://www.sciencedirect.com/science/article/pii/S0168900216302844

[5] M. Perez, M. S. Haro, I. Sidelnik, L. Tozzi, D. R. Brito, C. Mora, J. J. Blostein, M. G. Berisso, and J. Lipovetzky, "Commercial CMOS pixel array for beta and gamma radiation particle counting," in *Micro-Nanoelectronics, Technology and Applications (EAMTA), 2015 Argentine School of*, July 2015, pp. 11–16.

[6] E. Conti, P. Placidi, M. Biasini, L. Bissi, A. Calandra, B. Checcucci, S. Chiocchini, R. Cicioni, R. Di Lorenzo, A. C. Dipilato *et al.*, "Use of a CMOS image sensor for an active personal dosimeter in interventional radiology," *Instrumentation and Measurement, IEEE Transactions on*, vol. 62, no. 5, pp. 1065–1072, 2013.

[7] M. Pérez, J. J. Blostein, F. A. Bessia, A. Tartaglione, I. Sidelnik, M. S. Haro, S. Suárez, M. L. Gimenez, M. G. Berisso, and J. Lipovetzky, "Thermal neutron detector based on cots cmos imagers and a conversion layer containing gadolinium," *Nuclear Instruments and Methods in Physics Research Section A: Accelerators, Spectrometers, Detectors and Associated Equipment*, vol. 893, pp. 157 – 163, 2018. [Online]. Available: http://www.sciencedirect.com/science/article/pii/S0168900218303681

[8] J. H. Hubbell, N. I. o. S. S. M. Seltzer, and Technology, "Tables of x-ray mass attenuation coefficients and mass energy-absorption coefficients from 1 kev to 20 mev for elements z = 1 to 92 and 48 additional substances of dosimetric interest," *http://www.nist.gov/pml/data/xraycoef/*, 2004. [Online]. Available: http://www.nist.gov/pml/data/xraycoef/

[9] Alcalde Bessia F, Pérez M, Lipovetzky J, Piunno N. A. , Mateos H, Sidelnik I, Blostein J. J., Sofo Haro M. , Gómez Berisso M., "X-ray micrographic imaging system based on COTS CMOS sensors," *International Journal of Circuit Theory and Application*, p. in press, 2018.

[10] Open Source Computer Vision Library Project. Open source computer vision library. [Online]. Available: https://opencv.org/

[11] RaspiRaw Project. Raspiraw. [Online]. Available: https://github.com/6by9/raspiraw/

[12] *OV5647 datasheet*, Omnivission, 2009, version 1.0 – preliminary specification.

[13] E. Martin, T. Nuns, C. Virmontois, J.-P. David, and O. Gilard, "Proton and gamma-rays irradiation-induced dark current random telegraph signal in a 0.18-um CMOS image sensor," *Nuclear Science, IEEE Transactions on*, vol. 60, no. 4, pp. 2503–2510, Aug 2013.

[14] J. Bogaerts, B. Dierickx, G. Meynants, and D. Uwaerts, "Total dose and displacement damage effects in a radiation-hardened CMOS APS," *Electron Devices, IEEE Transactions on*, vol. 50, no. 1, pp. 84–90, 2003.